arXiv:0805.0506v1 [cond-mat.soft] 5 May 2008

Size dependent motion of nanodroplets on chemical steps

A. Moosavi, M. Rauscher, and S. Dietrich
Max-Planck-Institut für Metallforschung,
Heisenbergstr. 3, D-70569 Stuttgart, Germany, and
Institut für Theoretische und Angewandte Physik,
Universität Stuttgart, Pfaffenwaldring 57, D-70569 Stuttgart, Germany

(Dated: May 5, 2008)

Abstract

Nanodroplets on chemically structured substrates move under the action of disjoining pressure induced forces. A detailed analysis of them shows that even in the absence of long-ranged lateral variations of the effective interface potential, already the fact, that due their small size nanodroplets do not sample the disjoining pressure at all distances from the substrate, can lead to droplet motion towards the less wettable part of the substrate, i.e., in the direction opposite to the one expected on the basis of macroscopic wettability considerations.

PACS numbers: 68.08.Bc, 68.15.+e, 68.35.Ct

Chemically structured surfaces with their rather complex wetting properties [1] are not only ubiquitous in nature (e.g., beatles use them for harvesting drinking water out of fog [2]), they have also found important applications in a wide variety of processes ranging from ink-jet printing [3] and condensation heat transfer [4] to the so-called lab-on-a-chip concept for chemical analysis or biotechnology which, e.g., allows one to handle minute amounts of liquid containing DNA or proteins [5, 6]). In view of the richness of the corresponding wetting phenomena and in view of their importance, they have been intensively studied both experimentally [7, 8, 9, 10] and theoretically [11, 12, 13, 14, 15, 16, 17, 18, 19, 20, 21].

All the above mentioned applications of wettability patterns rely on the fact that the fluid placed on such a substrate will actually move towards the more wettable part [2, 4, 5, 6]. However, recently we could show, that nanodroplets near chemical steps can move in the opposite direction [21]. Due to the long range of dispersion forces of the van der Waals type, droplets residing on one side of the step perceive the different character of the other side even at finite distances from the step and move accordingly. Since the wetting properties (i.e., the equilibrium contact angles θ_{eq}) are determined by the interplay between both the long- *and* short-ranged interactions, the force resulting only from the long-ranged part is not necessarily directed towards the more wettable side [21].

In the present study we show that, in contrast to a droplet only *near* a chemical step, the direction of motion of a droplet positioned *on top of* a chemical step can depend on the size of the droplet and that, depending on the substrate characteristics, sufficiently small droplets move towards the less wettable side. For flat droplets this effect is robust, i.e., independent of the detailed properties of the chemical step (in contrast to the phenomena involving the approach towards chemical steps [21]) and it can be stronger as compared with this latter approach. This is true in particular for substrates the chemical patterns of which are generated by modifying the *short*-ranged part of the liquid-substrate interaction potential, as it is the case for many fabrication techniques (see, e.g., Ref. [10]). We strengthen this prediction by mesoscopic hydrodynamic calculations for two-dimensional droplets (i.e., filaments) and demonstrate its experimental relevance for polystyrene nanodroplets on silicon oxide, a system for which the actual material parameters are available.

We consider a droplet centered on a chemical step between two materials with coatings of different thickness and nature as illustrated in Fig. 1. As in Refs. [21, 22], we calculate the disjoining pressure (DJP) by integrating pair potentials over the substrate. In addition,

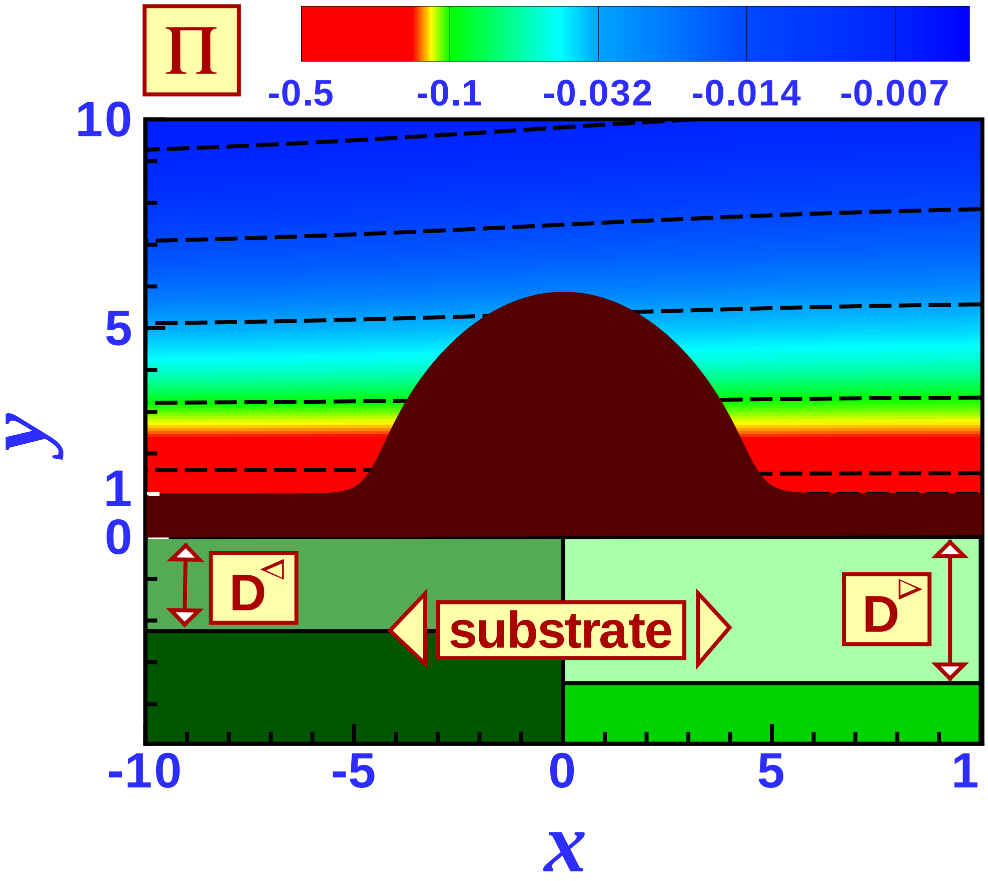

FIG. 1: A nanodroplet in contact with its corresponding equilibrium wetting film and located on top of a chemical step between two materials with coatings of different type and thickness. The contour and false color plot shows the vertically and laterally varying DJP for the example of two quarter substrates with different chemical composition but giving rise to the same equilibrium contact angle $\theta_{eq}^{\triangleleft} = \theta_{eq}^{\triangleright} = 90°$ (on the corresponding laterally homogeneous substrates) formed with the substrate surface. Due to the small size of the nanodroplet, its contact angles deviate from $\theta_{eq}^{\triangleleft}$ and $\theta_{eq}^{\triangleright}$, respectively. The corresponding parameter values are $C^{\triangleleft} = 1$, $B^{\triangleleft} = 7$, $D^{\triangleleft} = 1.227$, and $C^{\triangleright} = 1$, $B^{\triangleright} = 14$, $D^{\triangleright} = 2.251$; lengths and the DJP are measured in units of $b^{\triangleleft}$ and $\sigma/b^{\triangleleft}$, respectively; see the main text for definitions.

in order to demonstrate the robustness of the aforementioned effect, following Refs. [13, 18] we also use an approximate DJP which on each side of the chemical step equals the corresponding one of a laterally homogeneous substrate so that its lateral variation reduces to a discontinuity at $x = 0$.

A model chemical step as illustrated in Fig. 1 is composed of two different quarter spaces (edges) with each of them coated on its upper side with a different material. We model the intermolecular interactions between the liquid and the substrate as well as among the fluid particles via pairwise additive Lennard-Jones type intermolecular pair potentials, i.e., $V_{\alpha\beta}^{\triangleleft/\triangleright}(r) = M_{\alpha\beta}^{\triangleleft/\triangleright}/r^{12} - N_{\alpha\beta}^{\triangleleft/\triangleright}/r^6$, where $M_{\alpha\beta}^{\triangleleft/\triangleright}$ and $N_{\alpha\beta}^{\triangleleft/\triangleright}$ are material parameters for the left ($\triangleleft$) and right ($\triangleright$) half of the substrate, respectively, and α and β relate to either liquid (l), edge (e), or coating (c) particles. Following Ref. [23] the DJP $\Pi(x, y)$ of such a configuration can be calculated by integrating the liquid-substrate interactions over the substrate and by subtracting the integral of the liquid-liquid interaction potential over the volume occupied by the substrate. For the contribution of the left *e*dge without surface coating occupying $\Omega_e^{\triangleleft} = \{\mathbf{r} \in \mathbb{R}^3 | x \leq 0 \wedge y \leq 0\}$ one obtains

$$\Pi_e^{\triangleleft}(x, y) = \Delta M_e^{\triangleleft} I_{12}(x, y) - \Delta N_e^{\triangleleft} I_6(x, y), \tag{1}$$

with $I_n(x, y) = \int_{\Omega_e^{\triangleleft}} |\mathbf{r} - \mathbf{r}'|^{-n} \, d^3r'$, $\Delta M_e^{\triangleleft/\triangleright} = \rho_l^2 M_{ll} - \rho_l \rho_e^{\triangleleft/\triangleright} M_{el}^{\triangleleft/\triangleright}$, and $\Delta N_e^{\triangleleft/\triangleright} = \rho_l^2 N_{ll} - \rho_l \rho_e^{\triangleleft/\triangleright} N_{el}^{\triangleleft/\triangleright}$; ρ_l and $\rho_e^{\triangleleft/\triangleright}$ are the number densities of the liquid and the edge, respectively. The integrals $I_{12}(x, y)$ and $I_6(x, y)$ can be calculated analytically and can be used as suitable building blocks to obtain the contribution of the *c*oating layer of thickness $D^{\triangleleft}$ and of the right edge and its upper coating layer of thickness $D^{\triangleright}$. With these, the DJP of the chemical step is given by

$$\begin{aligned}
\Pi(x, y) = \Pi_{ce}^{\triangleleft} + \Pi_{ce}^{\triangleright} = \\
&\Delta M_c^{\triangleleft} \, [I_{12}(x, y) - I_{12}(x, y + D^{\triangleleft})] \\
&- \Delta N_c^{\triangleleft} \, [I_6(x, y) - I_6(x, y + D^{\triangleleft})] \\
&+ \Delta M_e^{\triangleleft} I_{12}(x, y + D^{\triangleleft}) - \Delta N_e^{\triangleleft} I_6(x, y + D^{\triangleleft}) \\
&+ \Delta M_c^{\triangleright} \, [I_{12}(-x, y) - I_{12}(-x, y + D^{\triangleright})] \\
&- \Delta N_c^{\triangleright} \, [I_6(-x, y) - I_6(-x, y + D^{\triangleright})] \\
&+ \Delta M_e^{\triangleright} I_{12}(-x, y + D^{\triangleright}) - \Delta N_e^{\triangleright} I_6(-x, y + D^{\triangleright}),
\end{aligned} \tag{2}$$

with $\Delta M_c^{\triangleleft/\triangleright} = \rho_l^2 M_{ll} - \rho_l \rho_c^{\triangleleft/\triangleright} M_{cl}^{\triangleleft/\triangleright}$ and $\Delta N_c^{\triangleleft/\triangleright} = \rho_l^2 N_{ll} - \rho_l \rho_c^{\triangleleft/\triangleright} N_{cl}^{\triangleleft/\triangleright}$. For $x \to -\infty$ one has $I_{12} \to \pi/(45\, y^9)$ and $I_6 \to \pi/(6\, y^3)$ so that far from the chemical step the DJP reduces to $\Pi_{ch}^{\triangleleft}$ and $\Pi_{ch}^{\triangleright}$ of a *c*oated laterally *h*omogeneous substrate on the left and right hand side, respectively. For small distances from the substrate surface, i.e., for $y \to 0$, the leading terms ($\sim \Delta M_c^{\triangleleft/\triangleright}\, \pi/(45\, y^9)$) in Eq. (2) are the terms $\Delta M_c^{\triangleleft}\, I_{12}(x, y)$ for $x < 0$ and $\Delta M_c^{\triangleright}\, I_{12}(-x, y)$ for $x > 0$, respectively. In order to have a wetting film of finite thickness $b^{\triangleleft/\triangleright}$, the disjoining pressure has to become very large at small distances from the substrate. Therefore, $\Delta M_c^{\triangleleft/\triangleright} \geq 0$ is a necessary condition for the occurrence of an equilibrium wetting film. But the other amplitudes can be positive or negative. In order to simplify the presentation we only consider the case $\Delta N_c^{\triangleleft/\triangleright} > 0$ as the relevant one for the experimental systems studied in Refs. [24, 25, 26]. Also by limiting ourself to coating layers thick compared with the wetting layer (see below) and to $|\Delta M_e^{\triangleleft/\triangleright}| \ll \Delta M_c^{\triangleleft/\triangleright}$, we neglect terms $\propto \Delta M_e^{\triangleleft/\triangleright}$ [25, 26]. For this system we introduce dimensionless quantities (marked by a star) such that lengths are measured in units of $b^{\triangleleft} = [2\Delta M_c^{\triangleleft}/(15\, \Delta N_c^{\triangleleft}|)^{1/6}$, which is the equilibrium wetting film thickness on a homogeneous flat substrate with the material of the left coating, and the DJP is measured in units of $\sigma/b^{\triangleleft}$ where σ is the liquid-vapor surface tension as an independent parameter. Thus the dimensionless DJP far from the edge ($x \to -/+\infty$) has the form

$$\Pi_{ch}^{*\triangleleft/\triangleright}(y_*) = C^{\triangleleft/\triangleright}\Bigg[\frac{{q^{\triangleleft/\triangleright}}^9}{{y_*}^9} - \frac{{q^{\triangleleft/\triangleright}}^9}{(y_* + D_*^{\triangleleft/\triangleright})^9} - \frac{{q^{\triangleleft/\triangleright}}^3}{{y_*}^3} + \frac{{q^{\triangleleft/\triangleright}}^3}{\left(y_* + D_*^{\triangleleft/\triangleright}\right)^3} - \frac{{q^{\triangleleft/\triangleright}}^3 B^{\triangleleft/\triangleright}}{\left(y_* + D_*^{\triangleleft/\triangleright}\right)^3}\Bigg], \quad (3)$$

with $C^{\triangleleft/\triangleright} = A^{\triangleleft/\triangleright}\, b^{\triangleleft}/\sigma$, $q^{\triangleleft/\triangleright} = b^{\triangleleft/\triangleright}/b^{\triangleleft}$ (i.e., $q^{\triangleleft} = 1$), and $B^{\triangleleft/\triangleright} = \Delta N_e^{\triangleleft/\triangleright}/\Delta N_c^{\triangleleft/\triangleright}$. The fully inhomogeneous and dimensionless DJP is obtained from Eq. (2) by replacing $\Delta M_c^{\triangleleft/\triangleright}$ by $45\, {q^{\triangleleft/\triangleright}}^9\, C^{\triangleleft/\triangleright}/\pi$, $\Delta N_c^{\triangleleft/\triangleright}$ by $6\, {q^{\triangleleft/\triangleright}}^3\, C^{\triangleleft/\triangleright}/\pi$, and $\Delta N_e^{\triangleleft/\triangleright}$ by $6\, {q^{\triangleleft/\triangleright}}^3\, C^{\triangleleft/\triangleright}\, B^{\triangleleft/\triangleright}/\pi$. In order to avoid a clumsy notation in the following we drop the stars. The macroscopic equilibrium contact angles $\theta_{eq}^{\triangleleft/\triangleright}$ far from the step are given by [27]

$$\cos\theta_{eq}^{\triangleleft/\triangleright} = 1 + \int_{y_0^{\triangleleft/\triangleright}}^{\infty} \Pi_{ch}^{\triangleleft/\triangleright}(y)\, dy. \quad (4)$$

The wetting film thickness $y_0^{\triangleleft/\triangleright}$ minimizes the effective interface potential $\omega^{\triangleleft/\triangleright}(y) = \int_y^\infty \Pi_{ch}^{\triangleleft/\triangleright}(y')\, dy'$ and both $\theta^{\triangleleft/\triangleright}$ and $y_0^{\triangleleft/\triangleright}$ can be expressed in terms of $C^{\triangleleft/\triangleright}$, $B^{\triangleleft/\triangleright}$, and $D^{\triangleleft/\triangleright}$[22, 27].

A typical example for the DJP at a chemical step is given in Fig. 1. The DJP $\Pi(x, y)$ obtained according to Eq. (2) is a continuous function of both x and y. Following Refs. [13,

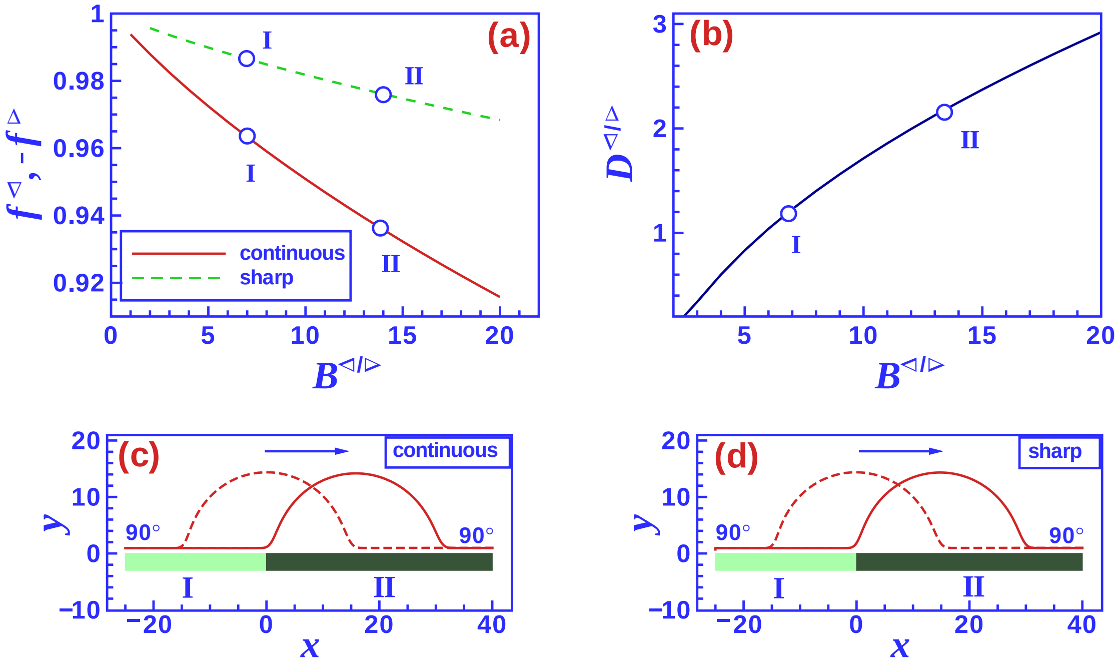

FIG. 2: (a): The continuous and the sharp DJP induced lateral force $f^{\triangleleft/\triangleright}$ originating from the left and the right part of the substrate, respectively, on a droplet of height a and basal width $2w$ with $a = w = 15$ centered on the chemical step as function of $B^{\triangleleft/\triangleright}$ which is varied together with $D^{\triangleleft/\triangleright}$ such that $\theta_{eq}^{\triangleleft} = \theta_{eq}^{\triangleright} = 90°$ (b). If the the left (right) substrate is chosen to correspond to I (II), $f = f^{\triangleleft} + f^{\triangleright} > 0$. The force per unit length is measured in units of σ. (c) and (d): Stokes dynamics of the same droplet on a chemical step between two substrates characterized by the materials parameters corresponding to points I ($C^{\triangleleft} = 1$, $q^{\triangleleft} = 1$, $B^{\triangleleft} = 7$, $D^{\triangleleft} = 1.227$) and II ($C^{\triangleright} = 1$, $q^{\triangleright} = 1$, $B^{\triangleright} = 14$, $D^{\triangleright} = 2.251$) in (a) and (b), respectively, for the continuous (c) and the sharp (d) DJP. The dashed line corresponds to the shape-relaxed initial state at time $t = 70$ and the solid lines to $t = 5000$ (c) and $t = 10500$ (d); times are given in units of $\mu b^{\triangleleft}/(C^{\triangleleft}\sigma)$. The droplets move to the right even though the equilibrium contact angles on both sides are equal.

18] we also consider the discontinuous approximation

$$\Pi_{dc}(x,y) = \begin{cases} \Pi_{ch}^{\triangleleft}(y) & \text{for } x < 0 \\ \Pi_{ch}^{\triangleright}(y) & \text{for } x > 0 \end{cases} \tag{5}$$

with $\Pi_{ch}^{\triangleleft/\triangleright}(y)$ defined in Eq. (3). In the following, we denote these two forms as "continuous" and "sharp", respectively.

The DJP induced lateral force on a two-dimensional droplet (i.e., the force per unit length

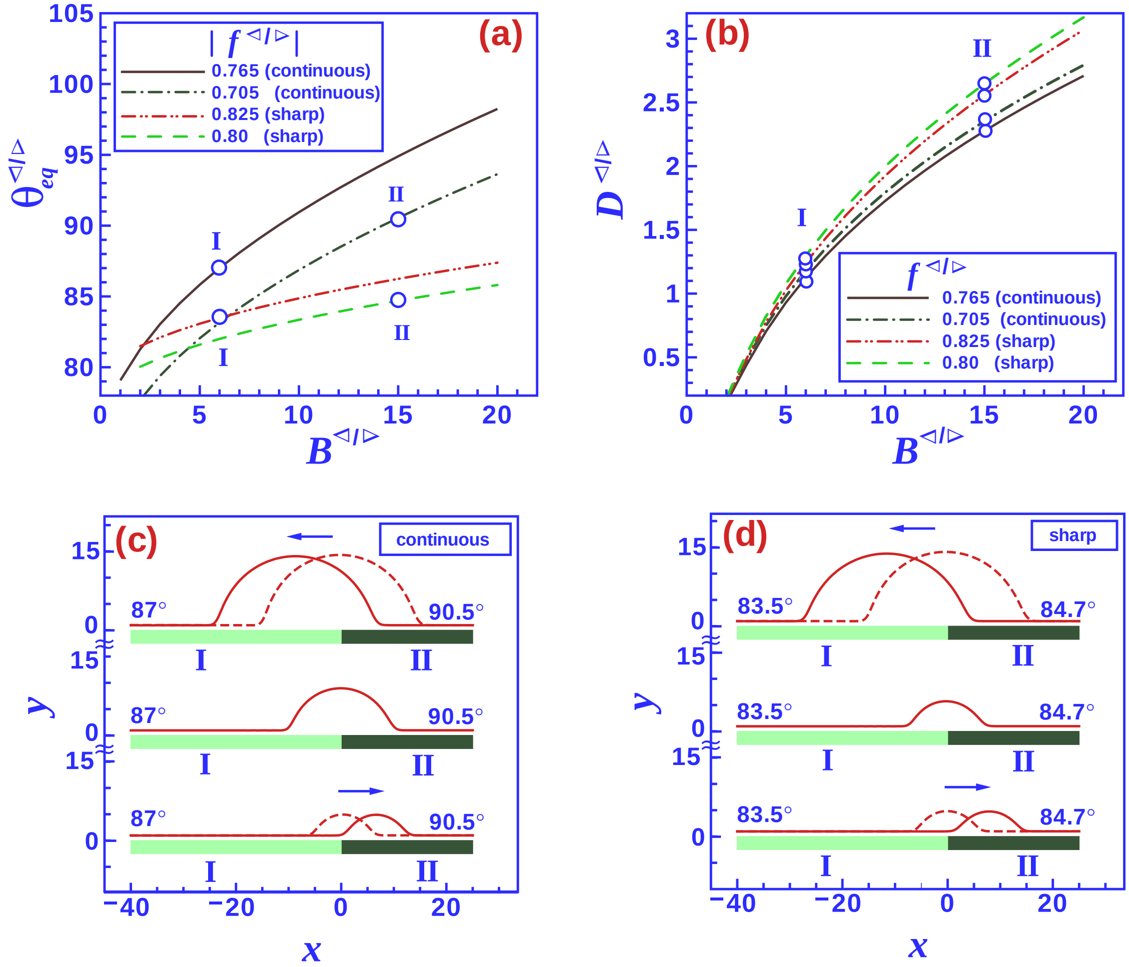

FIG. 3: (a), (b): Values of the parameters $B^{\lhd/\rhd}$ and $D^{\lhd/\rhd}$ and of the contact angle $\theta_{eq}^{\lhd/\rhd}$ for which the absolute value of the lateral force $|f^{\lhd/\rhd}|$ (originating from the left/right hand side of the substrate on a droplet of height a and width $2w$ with $a = w = 5$ centered on the chemical step) is equal to 0.705 or 0.765 (continuous) and 0.8 or 0.825 (sharp) in units of σ. (c) and (d): Results of the Stokes dynamics for the continuous (c) and sharp (d) DJP and for the parameter sets I (continuous: $B^{\lhd} = 6$, $D^{\lhd} = 1.1246$; sharp: $B^{\lhd} = 6$, $D^{\lhd} = 1.2414$) and II (continuous: $B^{\rhd} = 15$, $D^{\rhd} = 2.35$; sharp: $B^{\rhd} = 15$, $D^{\rhd} = 2.56$) in (a) and (b) for the left and the right side of the step, respectively ($C^{\lhd} = C^{\rhd} = 1$ and $q^{\lhd} = q^{\rhd} = 1$). The corresponding equilibrium contact angles with the substrate are indicated in the figures. The profiles correspond to times $t = 55$ (dashed lines) and 4000 (solid lines), in units of $\mu b^{\lhd}/(C^{\lhd}\sigma)$. From top to bottom $a = w = 15$, 9.38, and 5 for the continuous DJP and 15, 6, and 5 for the sharp DJP. Lengths are measured in units of $b^{\lhd}$.

on a liquid filament) spanning the chemical step is given by

$$f = \int_\Gamma \Pi(x,y)\, n_x\, ds = f^{\triangleleft} + f^{\triangleright}, \tag{6}$$

with Γ as the liquid-vapor interface and $n_x = -\frac{dy}{ds}$ as the x-component of the outward surface normal vector on Γ. Changing the integration variable from the contour length ds to dy we obtain for the forces due to the left and right hand part of the substrate, respectively,

$$f^{\triangleleft/\triangleright} = -\int_{y_0^{\triangleleft}}^{y_{\max}} \Pi_{ce}^{\triangleleft}(x<0)\, dy + \int_{y_0^{\triangleright}}^{y_{\max}} \Pi_{ce}^{\triangleleft}(x>0)\, dy, \tag{7}$$

with the droplet apex height $y_{\max}$. The first integral is the force on the left part ($x < 0$) of the droplet and the second integral the force on the right part ($x > 0$). For large droplets, i.e., for $y_{\max} \gg y_0^{\triangleleft/\triangleright}$, the upper limit of integration $y_{\max}$ can be approximated by ∞. If, in addition, the contact lines are at a large distance (as compared to $y_0^{\triangleleft/\triangleright}$) from the step, the main contribution to $f^{\triangleleft/\triangleright}$ stems from the part of the liquid-vapor interface in the vicinity of the left/right contact line where $\Pi_{ce}^{\triangleleft/\triangleright}(x,y) \approx \Pi_{ch}^{\triangleleft\triangleright}(y)$. Therefore for macroscopic drops one obtains $f^{\triangleleft/\triangleright} = \mp \int_{y_0^{\triangleleft/\triangleright}}^{\infty} \Pi_{ch}^{\triangleleft/\triangleright}(y) dy$ (which is independent of the droplet shape), and by using Eq. (4) one recovers the well known expression $f = \cos\theta_{eq}^{\triangleright} - \cos\theta_{eq}^{\triangleleft}$ (in units of σ) [7, 8, 11, 12].

The equilibrium contact angles $\theta_{eq}^{\triangleleft/\triangleright}$, which determine the force on macroscopic drops, are given by the integrals over $\Pi_{ch}^{\triangleleft/\triangleright}(y)$ from the equilibrium wetting film thickness to *infinity* (Eq. (4)). The force on a nanodroplet, however, does not depend on the values of the DJP for y larger than its height. Therefore, one can expect that (a) the force on nanodroplets depends on the size of the droplets and (b) that this force can be different for substrates with different DJP but with nonetheless the same equilibrium contact angle.

In order to estimate the force on a droplet spanning a chemical step — an unstable configuration for which one cannot resort to equilibrium shapes — we assume a simple analytical expression $y(x) = y_0 + a\left[1-(x/w)^2\right]^{|x|^{10}+1}$ for the droplet shape, which approximates a parabola of basal width $2\,w$ and height a which is smoothly connected with a wetting film of thickness y_0. In particular for flat droplets, the main contribution to f stems from the regions in the vicinity of the contact line, i.e., for relatively large distances from the chemical step, where $\Pi_{ce}^{\triangleleft/\triangleright}$ is well approximated by the DJP $\Pi_{ch}^{\triangleleft/\triangleright}$ of a homogeneous substrate.

For a droplet of size $a = w = 15$ Fig. 2(a) shows $f^{\triangleleft/\triangleright}$ as a function of $B^{\triangleleft/\triangleright}$ for substrates with $C^{\triangleleft/\triangleright} = 1$ and $D^{\triangleleft/\triangleright}$ chosen such that $\theta_{eq}^{\triangleleft} = \theta_{eq}^{\triangleright} = 90°$. Evidently, the droplet is too small to justify the sharp approximation, but in both models, $f^{\lhd}$ is monotonically decreasing. Although according to the above parameterization $y(x)$ the contact angles $\theta_{eq}^{\lhd/\rhd} = 90^\circ$ are fixed, the force depends on the substrate parameters such that due to $f^{\lhd} + f^{\rhd} \neq 0$ a droplet on top of a step between two sides with equal θ_{eq} but different chemical composition is driven to one or the other side of the step. A macroscopic drop does not move at all in this case. The chosen parameter values ($C^{\lhd} = C^{\rhd}$ and $q^{\lhd} = q^{\rhd} = 1$) correspond to two substrates with equal Hamaker constants. Therefore, to leading order in the distance from the step, the long-ranged lateral force on a droplet sitting next to (and not on top of) a chemical step is zero [21]. A careful analysis of the force on a slightly displaced droplet indicates, that the droplet stops when the trailing edge reaches the contact line. At this point the force changes sign.

This behavior is confirmed by mesoscopic hydrodynamic calculations based on the 2D Stokes equation for an incompressible liquid exposed to either the continuous or the sharp DJP (see Figs. 2(c) and (d)). This dynamics also takes into account the shape relaxation of the droplet. In dimensionless form the continuity and Stokes equations read $\boldsymbol{\nabla} \cdot \mathbf{u} = 0$ and $C^{\lhd}\, \boldsymbol{\nabla}^2 \mathbf{u} = \boldsymbol{\nabla} p$, respectively, where $\mathbf{u} = (u_x, u_y)$ is the velocity vector and p is the pressure [21]. With the viscosity μ, we use as the velocity and the time scale $C^{\lhd}\sigma/\mu$ and $\mu b^{\lhd}/(C^{\lhd}\sigma)$, respectively. Lengths and pressure are expressed in units of $b^{\lhd}$ and $\sigma/b^{\lhd}$, respectively. We have solved theses equations numerically with a standard biharmonic boundary integral method [28]. A no-slip boundary condition has been employed for the impermeable liquid-solid interface and a no-flux boundary condition was imposed at the left and right end of the system. At the liquid-vapor interface the tangential stresses are assumed to be zero and the normal stresses are balanced by surface tension and the DJP [28, 29] leading to

$$\mathbf{n} \cdot \tau \cdot \mathbf{n} = -\kappa + \Pi, \tag{8}$$

with the local mean curvature κ, the stress tensor τ, and the surface normal vector $\mathbf{n}$ pointing out of the liquid. Here, the parameterization of the droplet shape used in the force calculation was used as the initial configuration.

In Fig. 2 we show that the net force on a droplet can be non-zero even for equal macroscopic equilibrium contact angles on both sides. Since the contact angle as well as the force vary monotonically with the parameters, the net force is not necessarily directed towards the more wettable side of the step. As an example Figs. 3(a) and (b) show various values of $B^{\triangleleft/\triangleright}$ and $D^{\triangleleft/\triangleright}$ for which the absolute value of the lateral force on a nanodroplet (with dimensions $a = w = 5$) due to left/right side of the substrate is equal to $|f^{\triangleleft/\triangleright}| = 0.705$ or $|f^{\triangleleft/\triangleright}| = 0.765$ (continuous) and $|f^{\triangleleft/\triangleright}| = 0.8$ or $|f^{\triangleleft/\triangleright}| = 0.825$ (sharp). As function of these products $B^{\triangleleft/\triangleright}$ and $D^{\triangleleft/\triangleright}$, $\theta_{eq}^{\triangleleft/\triangleright}$ changes accordingly. For both values of $f^{\triangleleft/\triangleright}$ one can find system parameters such as the ones denoted as I and II so that the force $f_{\mathrm{I}}^{\triangleleft}$ from the less wettable side I is larger than $f_{\mathrm{II}}^{\triangleright}$ from the more wettable side II. Consequently, for such systems a droplet moves in the direction opposite to the one expected on the basis of the difference of contact angles. As in the example shown in Fig. 2, the force analysis for displaced droplets indicates that, independent of the droplet size, the droplets will stop their motion once the trailing contact line gets close to the chemical step. Both behaviors are also confirmed by the Stokes dynamics shown in Figs. 3(c) and (d): a small droplet of dimensions $a = w = 5$ moves towards the less wettable side, while a droplet of size $a = w = 15$ already behaves like a macroscopic droplet in the sense that it moves towards the more wettable side. For the system parameters chosen for Fig. 3 the critical size, for which the direction of motion in the Stokes dynamics changes sign, is found to be $a = w = 9.5$ and $a = w = 6$ in the case of the continuous and the sharp DJP, respectively.

Although the phenomenon described in Fig. 3, i.e., the motion towards larger contact angles, is not generic, it can be expected to appear in the extensively studied experimental system polystyrene (PS: $\sigma = 30.8\,\mathrm{mN/m}$, $\mu = 1200\,\mathrm{Pa\,s}$ [24]) on a silicon waver covered by SiO [25]. The experimental study reported in the Ref. [25] indicates that the DJP of this system, which is shown in the inset of Fig. 4(a) for two different thicknesses of oxide layers SiO (2.4 nm and 191 nm), can be represented by an expression of the form given in Eq. (3). The corresponding equilibrium contact angles are $\theta_{eq}^{\triangleleft} = 7.2^\circ$ ($C^{\triangleleft} = 0.054$, $B^{\triangleleft} = -5.91$) and $\theta_{eq}^{\triangleright} = 7.6^\circ$ ($C^{\triangleright} = 0.0155$, $B^{\triangleright} = -5.91$). A macroscopic droplet sitting on the chemical step should therefore move towards the side with the thinner oxide layer. The force calculation for droplets of varying sizes shows, however, a change of sign at a droplet height of about 7.5 nm for both the sharp and the continous DJP. In agreement with the force calculation, the Stokes dynamics calculations predict that a droplet of height a =5 nm moves towards the less wettable substrate. In the Stokes dynamics the droplet stops once its trailing contact line reaches the step. It covers about 80 nm in roughly 1100 s ($b^{\triangleleft} = 0.84$ nm), which should be experimentally observable.

In summary our study of the dynamics of droplets spanning chemical steps has revealed

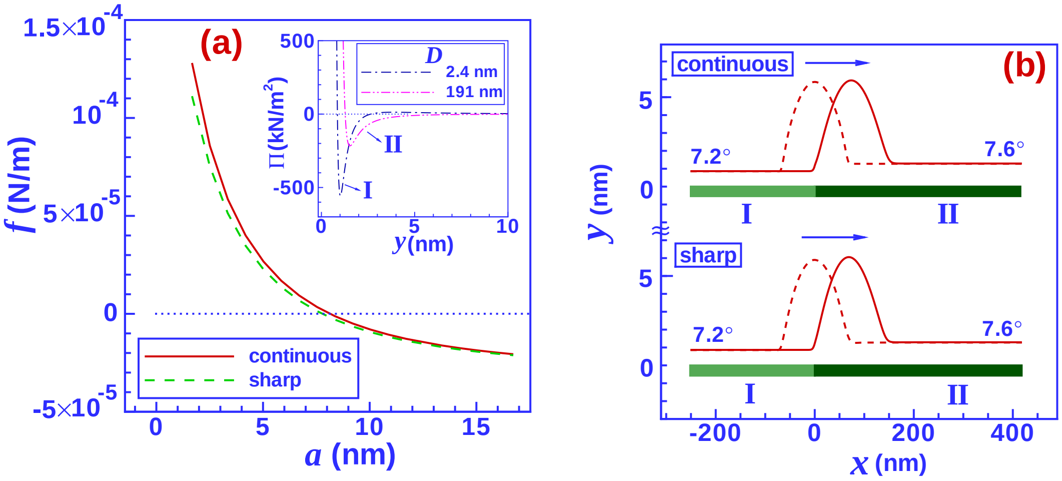

FIG. 4: (a) The DJP induced force of per length on a PS droplet centered on a chemical step composed of a Si wafer coated with oxide layers of two different thicknesses (I: $D^{\triangleleft} = 2.4$ nm, and II: $D^{\triangleright} = 191$ nm) as a function of the droplet height a. The ratio between the height a and the width w in the ansatz for the droplet shape is chosen to be $\tan(\alpha)$ with $\alpha = 7.5°$, i.e., in between the equilibrium contact angle 7.2° and 7.6° on the left and the right hand side, respectively. For $a \approx 7.5$ nm the force changes sign. The inset shows the DJP on both sides. (b) Stokes dynamics of a PS droplet with an initial height a =5 nm on a chemical step composed of coatings of type I on the left side and of type II on the right side. In (b) the profiles correspond to times $t = 0.1$ s (dashed lines) and to $t = 1050$ s and 1200 s (solid lines) for the continuous (top) and the sharp (bottom) DJP, respectively.

a qualitatively different behavior of nanodroplets as compared to macroscopic droplets [7, 8, 11, 12]. While the dynamic behavior of macroscopic droplets is solely determined by the difference of the equilibrium contact angles, the direction of motion of nanodroplets depends on their size and on details of the composition of the substrate. Nanodroplets can move towards one side of a chemical step under conditions for which macroscopic droplets either do not move at all or move to the opposite side of the step. Since most actual substrates exhibit nanoscale chemical heterogeneities, our results provide a basis for a better understanding of the dynamics of wetting phenomena, in addition to possible applications for handling, controlling, and guiding liquids in emerging nanofluidic devices. For instance, because the size, for which the direction of motion changes sign, also depends on the chemical composition of the droplets, this size selectivity has potential applications for droplet sorting by size or by composition in nanoscale fluidic devices.

M. Rauscher acknowledges DFG support under grant number RA 1061/2-1 (SPP 1164).

---

[1] S. Dietrich, *Fluids in contact with structured substrates*, in *New approaches to old and new problems in liquid state theory*, edited by C. Caccamo, J. P. Hansen, and G. Stell, NATO-ASI Series C, (Kluwer, Dordrecht, 1999) Vol. **C529**, p. 197 .

[2] A. R. Parker and C. Lawrence, Nature **414**, 33 (2001).

[3] J. Z. Wang, Z. H. Zheng, H. W. Li, W. T. S. Huck, and H. Sirringhaus, Nat. Mater. **3**, 171 (2004).

[4] S. Daniel, M. K. Chaudhary, and J. Chen, Science **291**, 633 (1992).

[5] G. Karniadakis, A. Beskok, and N. Aluru, *Microflows and Nanoflows: Fundamentals and Simulation*, 2nd ed. (Springer, NewYork, 2005).

[6] S. Dietrich, M. N. Popescu, and M. Rauscher, J. Phys. Condens. Matter **17**, S577 (2005).

[7] T. Ondarçuhu and M. Veyssié, J. Phys. II France **75**, 1 (1991).

[8] M. K. Chaudhury and G. M. Whitesides, Science **256**, 1539 (1992).

[9] J. Léopoldès and D. G. Bucknall, Europhys. Lett. **72**, 597 (2005).

[10] A. Checco, O. Gang, and B. M. Ocko, Phys. Rev. Lett. **96**, 056104 (2006).

[11] H. P. Greenspan, J. Fluid Mech. **84**, 125 (1978).

[12] E. Raphaël, C. R. Acad. Sci. Paris **306**, 751 (1988).

[13] L. W. Schwartz and R. R. Eley, J. Colloid Interf. Sci. **202**, 173 (1998).

[14] C. Bauer and S. Dietrich, Phys. Rev. E **60**, 6919 (1999).

[15] C. Bauer, S. Dietrich, and A. O. Parry, Europhys. Lett. **47** 474 (1999).

[16] J. Yaneva , A. Milchev, and K. Binder, J. Chem. Phys. **121**, 12632 (2004).

[17] M. Sprenger, F. Schlesener, and S. Dietrich, Phys. Rev. E **71**, 056125 (2005).

[18] U. Thiele, Phys. Rev. Lett. **97**, 204501 (2006).

[19] M. Cieplak, J. Koplik, and J. R. Banavar, Phys. Rev. Lett. **96**, 114502 (2006).

[20] A. Yochelis, E. Knobloch, and L. M. Pismen, Eur. Phys. J. E **22**, 41 (2007).

[21] A. Moosavi, M. Rauscher, and S. Dietrich, Langmuir **24**, 734 (2008).

[22] A. Moosavi, M. Rauscher, and S. Dietrich, Phys. Rev. Lett. **97**, 236101 (2006).

[23] M. O. Robbins, D. Andelman, and J. F. Joanny, Phys. Rev. A **43**, 4344 (1991).

[24] J. Becker, G. Grün, R. Seemann, H. Mantz, K. Jacobs, K. R. Mecke, and R. Blossey, Nat. Mater. **2**, 59 (2003).

[25] R. Seemann, S. Herminghaus, and K. Jacobs, Phys. Rev. Lett. **86**, 5534 (2001).

[26] R. Seemann, S. Herminghaus, and K. Jacobs, J. Phys.: Condens. Matter **13**, 4925 (2001).

[27] S. Dietrich, in *Phase Transitions and Critical Phenomena*, edited by C. Domb and J. L. Lebowitz (Academic, London, 1988), Vol. **12**, p. 1.

[28] M. A. Kelmanson, J. Eng. Math. **17**, 329 (1983).

[29] A. Oron, S. H. Davis, and D. G. Bankoff, Rev. Mod. Phys. **69**, 931 (1997).